JOURNAL OF CATALYSIS 33, 169–175 (1974)

EPR Study of the Nature and Removal of Iron(III) Impurities in Ammonium-Exchanged NaY-Zeolite

E. G. DEROUANE

Facultés Universitaires de Namur, Département de Chimie, 61, rue de Bruxelles, 5000-Namur, Belgium

AND

M. MESTDAGH AND L. VIELVOYE

Institut des Sciences de la Terre, Université Catholique de Louvain, 3030-Heverlee, Belgium

Received May 1, 1973

EPR studies of the Fe^{3+} impurity in NH_4-faujasite show that iron can be simultaneously present in the zeolite as three forms: Fe^{3+} species in the aluminosilicate framework, Fe^{3+} ions (possibly in $S_{I'}$ sites) acting as counterions, and Fe_3O_4 or another Fe^{3+} compound with strong exchange spin–spin interactions precipitated on the zeolite. All of these are incorporated in the zeolite in the course of its synthesis.

Chemical extraction and EPR data show that both the precipitated iron and the Fe^{3+} counterions can be easily removed from the zeolite. Substitutional Fe^{3+} cations in the aluminosilicate framework are probably also extracted, although this point is rather less conclusive. The chemical extraction procedure that is proposed provides a useful means of purifying commercial synthetic zeolites without altering their crystallographic structure.

INTRODUCTION

Because of the importance of commercial zeolites in adsorption and catalysis, it is necessary to understand the role of impurities present in these materials, the effect they may have on the intrinsic zeolite activity and whether or not they can be removed without altering the basic zeolite framework. This paper is concerned with iron impurity ions.

In a recent paper, McNicol and Pott (*1*) have shown unambiguously that Fe^{3+} species in faujasite and mordenite may be substituted in the aluminosilicate framework. In the same work, and in an earlier study by Singer and Stamires (*2*), wide electron spin resonance signals were also observed in heat-treated NH_4-zeolites and attributed to Fe_3O_4 or Fe/Al species precipitated in the zeolite cavities during the deammoniation process. A third possibility is that Fe^{3+} cations (presumably hydroxylated) occupy exchange sites (*1*).

Mössbauer spectroscopic studies by Boudart and co-workers (*3–5*) on iron-exchanged Y-zeolites have enabled the location of the exchanged Fe^{3+} cations to be at least partially defined. For samples heat-treated at 400°C, the Fe^{3+} cations occupy $S_{I'}$ sites and achieve almost perfect tetrahedral coordination with the O_3 oxygens and one oxygen atom bridging two neighboring Fe^{3+} cations. At room temperature, for samples that have not been evacuated, the possibility exists of forming bridged Fe^{3+}–O^{2-}–Fe^{3+}–OH^- entities involving Fe^{3+} ions located at the center of adjacent hexagonal prisms.

The role of retained water is probably a determining factor for the activity of the zeolites (*6–8*). A related, important factor is the mobility of framework hydroxyl groups (or protons) (*9*), which in principle can be studied by the pulsed NMR technique (*10*). Unfortunately, as shown, for example, by Michel (*11*), the determination of the proton relaxation times values that lead directly to the evaluation of the proton mobility is rather difficult in the presence of paramagnetic impurities, even if those are present in very small amount.

As will be shown in this study, a commercial faujasite may contain as much as nearly 2000 wt.-ppm Fe^{3+} (expressed in Fe_2O_3 units), of which about 1000 wt.-ppm correspond to Fe^{3+} ions in cationic exchange sites; these actually amount roughly to 1.5% of the total cationic exchange capacity of the Y-zeolitic lattice.

These considerations show clearly the interest of locating, and if possible removing, polyvalent or paramagnetic cations in the zeolites when basic catalytic activity or structural studies are undertaken.

EXPERIMENTAL METHODS

Materials

A commercial Linde SK-40 zeolite (Y-type faujasite, lot number 3606-289) was used as a starting material. The NH_4^+-exchanged form was prepared by batch exchange in NH_4Cl 1 *M* at 25°C for 48 hr. The chemical composition of the anhydrous compound was $(NH_4)_{38}Na_{16}Al_{54}Si_{138}O_{384}$, corresponding to a Si:Al ratio of 2.58 and a percentage of exchange of 70%. At room temperature, the number of water molecules per the above molecular unit was 280. A nuclear activation analysis indicated the presence of Fe^{3+}, which, expressed as Fe_2O_3, amounted to 1750 ± 50 wt.-ppm.

Chemical Extraction Procedure

Two-hundred milligrams of zeolite were added to 7 ml distilled water and 1 ml 10% NaCl solution in a 15-ml centrifugation tube. After addition of 50 mg $Na_2S_2O_4$, the mixture was heated for 15 min at 70°C without agitation and centrifuged. The liquid was then transferred to a 25-ml flask, and the amount of Fe^{2+} was determined by colorimetry using the method described by Charlot (*17*). The remaining solid was dried in air at 40°C.

No iron was detected in a blank sample, and a 20-ppm Fe^{3+} standard (Mohr salt) gave 20 ppm iron extracted as Fe^{2+}. X-Ray spectra taken on a Philips-Norelco 1010 diffractometer showed no alteration of the zeolite structure after the iron extraction treatment.

Instrumental Techniques

EPR measurements were made on a X-band E-12 Varian spectrometer, using 100 kHz modulation, at 298°K, 77°K, or at 4.2°K using a liquid He cryostat especially designed for low-temperature work with a large sample access cavity.

RESULTS AND DISCUSSION

Nature and Location of Fe^{3+} Species in Undegassed NH_4Y-Zeolites

Figures 1 and 2 show EPR spectra of the undegassed NH_4Y-zeolite. Fairly identical spectra were obtained from a Linde SK-40 NaY faujasite (Lot number 3607-411, 952 wt.-ppm Fe_2O_3). This implies that our ma-

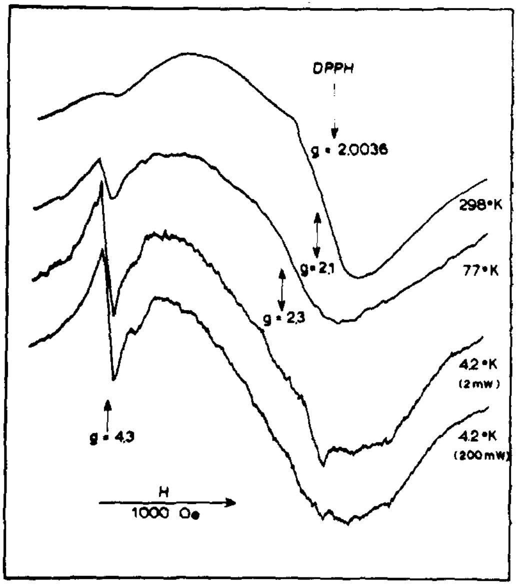

FIG. 1. EPR spectra at various temperatures of Fe^{3+} in undegassed NH_4Y-zeolite. Microwave power levels for the 4.2°K spectra are indicated in parentheses.

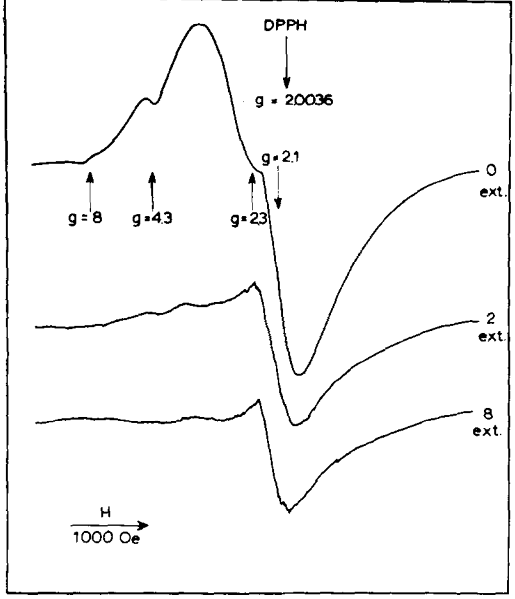

FIG. 2. EPR spectra at 298°K of Fe^{3+} in NH_4Y-zeolites after various numbers of extraction steps as indicated on the spectra.

terial had not been contaminated during its handling or exchanging with NH_4Cl and suggests that the case we are dealing with is probably not unique.

Three EPR signals may be distinguished: a broad and symmetrical signal at g_{eff} = 2.3 (1300 Oe width) and two narrower signals at g_{eff} = 4.3 and 2.1 (widths of 125 and 250 Oe, respectively).

The temperature dependence of the EPR spectrum (Fig. 1) shows clearly that the signals observed at g_{eff} = 4.3 and g_{eff} = 2.3 correspond to different species. On the other hand, from the spectra recorded at 4.2°K with appreciably different incident microwave powers, it is seen that the g_{eff} = 2.1 line saturates more readily than the g_{eff} = 4.3 line. Figure 2, which shows the EPR spectra recorded at 298°K after an increasing number of extraction steps, also indicates that a distinction must be made between the g_{eff} = 2.3 and the g_{eff} = 2.1 lines. The three EPR signals thus correspond to distinct paramagnetic species. From the estimated concentration of unpaired spins, the only chemically detectable paramagnetic impurity that could account for a resonance with this intensity is iron, i.e., Fe^{3+}. Other impurities such as titanium or chromium are also present, but at a lower concentration level, and their paramagnetic forms, Ti^{3+} and Cr^{3+}, would show EPR signals below $g = 2$ (the free electron g-value). Those have not been observed.

Fe^{3+} can be present in the zeolites in a variety of forms, namely (i) in the aluminosilicate framework with distorted tetrahedral coordination (*1*), Fe_S^{3+}, (ii) in exchangeable sites, Fe_C^{3+}, and (iii) as a more or less amorphous oxidic, hydroxidic, or salt material precipitated on the zeolite (*1*, *2*), Fe_P^{3+}.

Table 1 summarizes the characteristic parameters of the identified Fe^{3+} species, at different temperatures.

The broad line observed at g_{eff} = 2.3 is similar in its EPR characteristics and temperature behavior to that previously reported in the NH_4Y heat-treated zeolites (*1*, *2*) and attributed to a ferromagnetic material of Fe(III). Similarly, we identify this signal to Fe/Al oxide or hydroxide microcrystallites precipitated on the zeolite in the course of its industrial synthesis. This accounts in addition for their fast removal by chemical agents. This species will be referred to as Fe_P^{3+}.

The small intensity line observed at g_{eff} = 4.3 and the corresponding low-field shoulder at g_{eff} = 8.5 have been previously observed by McNicol and Pott (*1*) for Fe^{3+} in the hydrated forms of both NaY and

TABLE 1

EPR PARAMETERS FOR THE DIFFERENT TYPES OF Fe^{3+} SPECIES OBSERVED IN NH_4-FAUJASITE

Nature	Temperature (°K)	g-value (±0.05)	Width[a] (Oe)
Fe_C^{3+}	298	2.08	250
	77	2.12	150
	4.2	2.10	140
Fe_S^{3+}	298	4.30	125
	77	4.23	110
	4.2	4.23	100
Fe_P^{3+}	298	2.30	1280
	77	2.30	1450
	4.2	2.30	1550

[a] Approximate values within 5%.

NH_4Y zeolites. Such low-field signals were also reported for Fe^{3+} in glasses (*12*, *14*) and kaolins (*13*). They arise in C_{2v} symmetry, which corresponds to rhombically distorted octahedral (MA_4B_2, MA_3B_3) or tetrahedral (MA_2B_2) environments as discussed by various authors (*14*, *15*). In agreement with McNicol and Pott (*1*), this species is assigned to Fe^{3+} ions in the aluminosilicate framework, i.e., Fe_S^{3+}.

A third species, Fe_C^{3+}, is characterized by $g_{eff} = 2.1$. It is the only one we detected in purer zeolitic materials (prepared in a conventional way in our laboratories, about 80 wt.-ppm Fe^{3+} as Fe_2O_3) for which all the Fe^{3+} impurities are in exchange sites as shown by chemical exchange with a NaCl solution. As seen from Fig. 2, it is extracted, but at a smaller rate than the Fe_P^{3+} species, by chemical agents. To account for g-values near 2, the Fe^{3+} ions must be in a rather symmetrical environment (*16*). Possible configurations where both D and E are small are either a regular octahedron (MA_6, O_h) or tetrahedron (MA_4, T_d), or a distorted octahedron with C_{3v} symmetry (MA_3B_3) (*14*). It is also known, from previous work on kaolins (*13*), that distortions from ideal octahedral symmetry by flattening of shared octahedral edges may lead to Fe^{3+} EPR signals near $g = 2$.

Fe^{3+} ions in accessible exchange sites of the hydrated Y-zeolites may be octahedrally coordinated in S_I sites (hexagonal prism), tetrahedrally coordinated in $S_{I'}$ sites (*5*), or in a distorted octahedral coordination (C_{3v}) such as that found for various exchange sites (I′,II,II′) in the hydrated materials.

The extraction process that is used involves primarily a reduction of Fe^{3+} in Fe^{2+} by the $S_2O_4^{2-}$ anion. Then, eventually after a partial complexation of Fe^{2+} by the $S_2O_4^{2-}$ ions in excess, Fe^{2+} is exchanged quantitatively by the Na^+ ions provided by a NaCl solution of very high ionic force. Because of the large size of the $S_2O_4^{2-}$ ion and the important steric hindrance to its penetration in the hexagonal prisms, one would not expect Fe^{3+} ions in S_I sites to be removed so easily. On the other hand, a nearly regular tetrahedral coordination of Fe^{3+} cations in $S_{I'}$ sites (*5*) is rather unlikely in materials that have not been degassed or heated at near 400°C.

Various structural data (*18*, *22*, *23*) indicate that in the hydrated compound, hydrolyzed trivalent cations, such as La^{3+}, occupy I′ rather than II sites, these in turn being strongly preferred to type-I sites. EPR studies of hydrated synthetic zeolites containing Mn^{2+} and various other cations lead essentially to the same conclusions (*19–21*).

Hence, we think that the Fe_C^{3+} species might correspond to octahedrally coordinated Fe^{3+} ions with C_{3v} symmetry, similar, for example, to those located in $S_{I'}$ sites, which can be coordinated to three O_3 oxygens and three OH^- groups or water molecules present in the sodalite cage. Other possibilities exist that are less probable on the basis of a comparison with the data for the La^{3+} ion: they correspond to similar C_{3v} symmetry arrangements in type II or type II′ sites.

The conclusion, therefore, is that Fe^{3+} species can be present simultaneously in undegassed Y-type zeolites in three configurations: i.e., (i) Fe^{3+} substitutional ions in the aluminosilicate framework, (ii) Fe^{3+} ions in exchange sites, and (iii) precipitated Fe^{3+}-containing species on the zeolite structure, all of these being incorporated in the zeolite in the course of its synthesis.

Chemical Extraction of the Fe^{3+} Impurities

Chemical extraction of the Fe^{3+} impurities was performed by repeating the elementary extraction step described in the experimental section.

Figure 3 shows the amount of Fe^{3+} removed (expressed as Fe_2O_3, in wt.-ppm) for various amounts of sample, with and without stirring, as a function of the number of extraction steps. The extraction of Fe^{3+} from a 1-g sample (C) was performed with five times as much reactant as for the 0.2-g samples (A and B). From the general shape of the extraction curves, one concludes that there are two extraction processes: a fast process (I) for a number of steps under 4 and a slow and quite linear process (II) that is present from the very

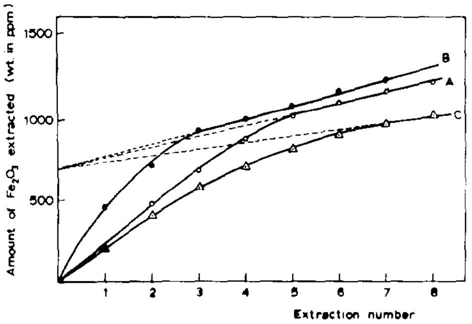

FIG. 3. Effect of stirring and sample amount on extraction efficiency. A(○): 0.2 g, no stirring; B(●): 0.2 g, with stirring; and C(△): 1 g, no stirring.

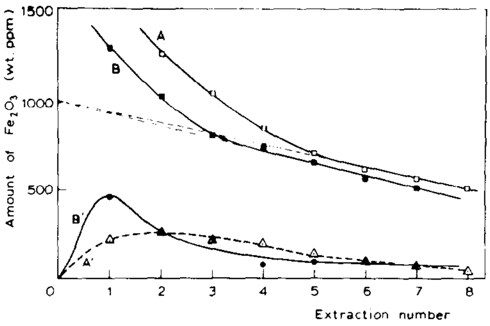

FIG. 4. Amount of Fe^{3+} extracted (in wt.-ppm Fe_2O_3) vs cumulative extraction steps. A: 0.2 g, no stirring; B: 0.2 g, with stirring. A′(△) and B′(●) show the amount extracted at each step. A(□) and B(■) are cumulative values with respect to the remaining Fe^{3+} (Fe_P^{3+} + Fe_C^{3+}).

first extraction step. It is clear from the EPR data (Fig. 2) that process I corresponds to the removal of the precipitated iron, Fe_P^{3+}, while process II must be assigned to the removal of Fe_C^{3+}, possibly by cationic exchange. Hence, all the linear parts of the extraction curves must extrapolate to the same ordinate value, which corresponds to the amount of Fe^{3+} *which is not extracted* by process II, i.e., the precipitated iron on the zeolite, Fe_P^{3+}. This is found to be 700 ± 50 wt.-ppm Fe_2O_3. The effect of stirring and that of the initial sample amount are also found to be smaller on process II than on process I, in accordance with their assignments. Note also that stirring or a decreasing amount of starting material increase the extraction rate of the Fe_P^{3+} species, as expected.

Figure 4 shows plots of the amount of Fe^{3+} removed at each step, with and without stirring, and the cumulative curves representing the respective amounts of residual Fe^{3+} in the zeolite (Total Fe^{3+} minus Fe^{3+} extracted as determined from chemical analysis). Again, it is concluded that stirring increases the rate of process I and has little effect on process II. Extrapolation of the linear parts of the cumulative plots leads in this case to the amount of Fe^{3+} *that is extracted* by process II, i.e., Fe_C^{3+} and eventually Fe_S^{3+}. This is found to be 1020 ± 30 wt.-ppm (expressed as Fe_2O_3).

In order to ascertain more quantitatively the nature of the extraction processes and to determine whether or not Fe_S^{3+} could be removed, a quantitative comparison has been established between EPR and chemical analysis data as shown in Fig. 5 and Table 2. After eight extractions, as seen from Fig. 2, only one type of signal is observed, at g_{eff} = 2.1, i.e., Fe_C^{3+}. Hence, its intensity can be normalized to the total amount of residual Fe^{3+} impurities as determined from chemical analysis (522 wt.-ppm Fe_2O_3) and the amount of Fe_C^{3+} re-

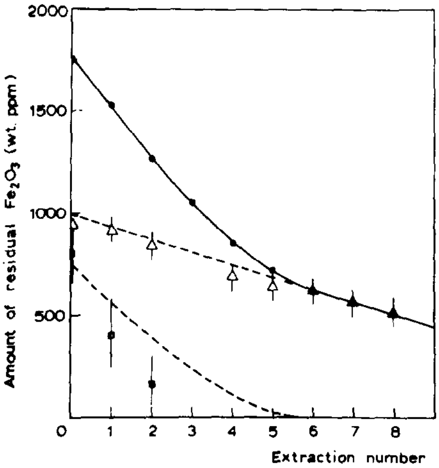

FIG. 5. Amount of residual Fe^{3+} (Fe_P^{3+} + Fe_C^{3+}, in wt.-ppm Fe_2O_3) vs cumulative extraction steps. ——(●): residual Fe^{3+} content from chemical analysis; △: residual Fe_C^{3+} from EPR data; ■: residual Fe_P^{3+} from EPR data: and ---: extrapolated or calculated variations.

TABLE 2

Fe^{3+} EXTRACTION FROM NH_4-FAUJASITE

			Residual Fe_2O_3 amount from EPR[b] (wt-ppm)		
Number of extractions (1)	Amount of Fe_2O_3 extracted[a] (wt-ppm) (2)	Residual amount of Fe_2O_3 (wt-ppm) (3)	Fe_P^{3+} (4)	Fe_C^{3+} (5)	Total (6)
0	0	1750	(802)	948	(1750)
1	221	1529	401	909	1310
2	486	1264	156	836	992
3	694	1056	—	—	—
4	895	855	—	689	689
5	1026	724	—	642	642
6	1124	626	—	623	623
7	1189	561	—	569	569
8	1228	522	—	(522)	(522)

[a] From chemical analysis (colorimetry).

[b] All Fe^{3+} concentrations in units of wt.-ppm Fe_2O_3; EPR intensity calibration points are indicated in parentheses.

maining after each extraction can easily be monitored by evaluation of the intensity of the $g_{eff} = 2.1$ line (column (5) in Table 2 and open triangles in Fig. 5). This is found to follow quantitatively the expected linear variation for process II (dashed line) and one determines about 948 ± 50 wt.-ppm Fe_C^{3+} (in Fe_2O_3 units) in the untreated material.

On the other hand, it is known that the amount of Fe_S^{3+}, in our case, is rather small, as seen from the relative intensity of the EPR line at $g_{eff} = 4.3$ *in the room temperature EPR spectra.* Neglecting it as a first approximation, the amount of Fe_P^{3+} in our fresh zeolite must be 802 ± 50 wt.-ppm Fe_2O_3. This provides a way for calibrating the intensity of the $g_{eff} = 2.3$ resonance line in the starting material, and, hence, it is possible to monitor by EPR the progressive extraction of Fe_P^{3+} (column (4) in Table 2 and black squares in Fig. 5). The calculated variation (dashed line) is also shown. Again, one finds a quite good agreement within experimental error, although it is not so nice as for Fe_C^{3+}. This may be because of the large errors involved in the shape and intensity evaluations of broad and weak signals such as those observed for the Fe_P^{3+} species after more than two extractions.

Although it cannot be ascertained quantitatively because of the weakness of this contribution, the fact that EPR calculated values for the total residual amount of Fe^{3+} (column (6) in Table 2) are always smaller than (or equal to) values determined from chemical analysis (column (3) in Table 2) indicates that the Fe^{3+} substitutional cations in the zeolite framework are probably also removed. One expects that this type of impurity should be extracted by reducing agents such as $Na_2S_2O_4$. However, this point should be taken with caution, since X-ray diffraction will not be sensitive to the destruction of a very small part of the zeolite framework and, in addition, a $g_{eff} = 4.3$ signal was sometimes observed even after seven extraction steps. From the extrapolated value based on chemical analysis ($Fe_C^{3+} + Fe_S^{3+}$, 1020 wt.-ppm Fe_2O_3) and the EPR determined value for Fe_C^{3+} (948 wt.-ppm Fe_2O_3), the amount of Fe_S^{3+} in the fresh zeolitic material is found to be 70 ± 50 wt.-ppm (in Fe_2O_3 units).

Hence, it is concluded that the chemical analysis and extraction data strongly support the following assignments of the nature and location of the Fe^{3+} species. Fe^{3+} precipitated on the zeolite is readily extracted while Fe^{3+} in exchange cationic sites is removed more slowly. Substitutional Fe^{3+} cations in the aluminosilicate framework are probably also extracted, although this latter point is rather less conclusive. The combination of EPR and chemical data enable the determination of the amount of Fe^{3+} impurities in the various proposed configurations and the chemical extraction procedure provides a useful means of purifying commercial synthetic zeolites.

ACKNOWLEDGMENTS

Thanks are due to Professors J. J. Fripiat and J. B. Uytterhoeven for valuable discussions. We also thank Professor G. Deconninck for the analyses made at the "Laboratoire d'Analyse par Réaction Nucléaire" and Professor A. Herbillon for suggestions on the chemical extraction procedure. One of us (E.G.D.) would like to thank the "Fonds National de la Recherche Scientifique" (Belgium) for his former "Chargé de Recherches" position. This work was supported by a grant of the "Fonds de la Recherche Fondamentale Collective."

REFERENCES

1. McNicol, B. D., and Pott, G. T., *J. Catal.* **25**, 223 (1972).
2. Singer, L. S., and Stamires, D. N., *J. Chem. Phys.* **42**, 3299 (1965).
3. Delgass, W. N., Garten, R. L., and Boudart, M., *J. Chem. Phys.* **50**, 4603 (1969).
4. Delgass, W. N., Garten, R. L., and Boudart, M., *J. Phys. Chem.* **73**, 2970 (1969).
5. Garten, R. L., Delgass, W. N., and Boudart, M., *J. Catal.* **18**, 90 (1970).
6. Ward, J. W., *J. Catal.* **10**, 34 (1968).
7. Kemball, C., and McCosh, R., *Proc. Roy. Soc. London* **A321**, 249 (1971).
8. Jacobs, P. A., and Uytterhoeven, J. B., *J. Chem. Soc. Faraday Trans. I*, **69**, 373 (1973).
9. Hirschler, A. E., Neikam, W. C., Barmby, D. S., and James, R. L., *J. Catal.* **4**, 628 (1965).
10. Resing, H. A., *Advan. Molec. Relax. Processes* **3**, 199 (1972).
11. Michel, D., *Z. Naturforsch.* **22A**, 1751 (1967).
12. Castner, T., Newell, G. S., Holton, W. C., and Slichter, C. P., *J. Chem. Phys.* **32**, 668 (1960).
13. Angel, B. R., and Hall, P. L., *Intern. Clay. Conf. Madrid* 1972; Reprints Vol. 1, p. 71.
14. Loveridge, D., and Parke, S., *Phys. Chem. Glasses* **12**, 19 (1971).
15. Griffith, J. S., *Molec. Phys.* **8**, 213, 218 (1964).
16. Low, W., *Phys. Rev.* **105**, 792 (1957).
17. Charlot, G., "Les Méthodes de Chimie Analytique." Masson, Paris, 1966, p. 741.
18. Bennett, J. M., and Smith, J. V., *Mat. Res. Bull.* **4**, 343 (1969).
19. Barry, T. I., and Lay, L. A., *J. Phys. Chem. Solids* **29**, 1395 (1968).
20. Barry, T. I., and Lay, L. A., *J. Phys. Chem. Solids* **27**, 1821 (1966).
21. Tikhomirova, N. N., Nikolaeva, I. V., Demkin, V. V., Rosolovskaya, E. N., and Topchieva, K. V., *J. Catal.* **29**, 105 (1973).
22. Smith, J. V., Bennett, J. M., and Flanigen, E. M., *Nature*, **215**, 241 (1967).
23. Olson, D. H., Kokotailo, G. T., and Charnell, J. F., Colloid Symposium, Buffalo, N. Y. (1967); *Nature* **215**, 270 (1967).